Check for updates

# A 3D printable synthetic hydrogel as an immobilization matrix for continuous synthesis with fungal peroxygenases†

Lars-Erik Meyer, [iD] [a] Dorottya Horváth,[a] Sonja Vaupel, [iD] [b] Johanna Meyer, [iD] [b] Miguel Alcalde [iD] [c] and Selin Kara [iD] *[ab]

**Enzyme immobilization is the key to an intensified bioprocess that allows recycling of the heterogenized enzyme and/or continuous biocatalytic production. In this communication, we present a case study for enzyme immobilization in a novel, 3D printable synthetic hydrogel and its use in continuous oxidation reactions. Immobilization resulted in an average immobilization yield of 6.1% and continuous synthesis was run for 24 hours with a space–time yield of $3.1 \times 10^{-2}$ g L$^{-1}$ h$^{-1}$.**

The exploration for novel immobilization materials plays an essential role in research, enabling biotransformations in continuous flow,[1a–c] biocatalysis in non-conventional media (BNCM),[2a–c] or process intensification as a whole.[3a–c] In general, enzymes work best in aqueous media due to their origin in prokaryotic or eukaryotic cells. Therefore, a possible immobilization procedure for a continuous BNCM approach should include a carrier material that stabilizes the enzyme by maintaining its hydration shell.

Hydrogels are crosslinked hydrophilic three-dimensional polymeric networks that do not dissolve in water but, conversely, absorb large amounts of water while preserving their well-defined scaffolds. Typical hydrogel characteristics combine biocompatibility,[4a,b] antimicrobial behavior,[5] self-healing,[6] as well as tunable mechanical,[7] and swelling properties.[8] Since hydrogels can provide the desired aqueous microenvironment for enzymes, researchers began to use hydrogels as immobilization matrices.[9] Here, mostly hydrogels from renewable resources were used: polysaccharides such as (i) agarose, (ii) alginate, (iii) carrageenan, (iv) cellulose,

(v) chitosan, (vi) hyaluronic acid, and (vii) starch, or proteins such as (i) collagen, (ii) fibrin, and (iii) gelatin. In recent years, also novel developments were reported in the literature focusing on the 3D printing of hydrogel-immobilized enzymes. As one of the selected examples, Maier *et al.* fabricated grid-structured agarose-based hydrogel scaffolds into which three types of thermostable enzymes (an esterase, an alcohol dehydrogenase, and a decarboxylase) were immobilized. Here, the modules were constructed by rapid prototyping and used in a biocatalytic flow system.[10] Croci *et al.* carried out a reductive amination from benzaldehyde substrate by co-immobilized amine dehydrogenase and formate dehydrogenase. The authors immobilized the enzymes in an agarose hydrogel cast in a 3D-printed mold and applied them in a continuous flow micro-reactor achieving a space–time-yield of 7.4 g L$^{-1}$ h$^{-1}$. Their study presented a simple and efficient solution for implementing 3D-printed hydrogel units with pre-determined structure in continuous flow.[11] Wenger *et al.* compared bioinks of agar and agarose containing the thermostable esterase 2 from *Alicyclobacillus acidocaldarius* with respect to their applicability for extrusion-based rapid prototyping. Their setup was favorable for the fabrication of prints with a clean and defined structure. The agarose inks with 4.5% polymer showed no leaching and convenient printability, making them ideal for bioreactor 3D printing.[12] Wang *et al.* reported the efficient synthesis of a bis(acyl)phosphane oxide (BAPO) photoinitiator in a one-pot system, that they applied in the photopolymerization of polyethylene glycol (PEG)-based hydrogels. A digital light processing printer was used and hydrogels with a gyroid structure were successfully photopolymerized under 460 nm.[13] We reviewed recent developments in enzyme immobilization in natural and synthetic hydrogels and highlighted the positive implications for efficient and sustainable biocatalysis.[14] In addition, we published novel 3D printable synthetic hydrogel materials and carefully investigated their properties. Here, we were able to demonstrate the first 3D printing attempts, using a mild photoinduced lithography technique to initiate the polymerization process.

[a] *Biocatalysis and Bioprocessing Group, Department of Biological and Chemical Engineering, Aarhus University, Gustav Wieds Vej 10, 8000 Aarhus, Denmark. E-mail: selin.kara@bce.au.dk*

[b] *Institute of Technical Chemistry, Leibniz University Hannover, Callinstr. 5, 30167 Hannover, Germany. E-mail: selin.kara@iftc.uni-hannover.de*

[c] *Miguel Alcalde Laboratory, Institute of Catalysis, ICP-CSIC, Cantoblanco, 28049, Madrid, Spain*

In this communication, we present our idea to immobilize the enzyme unspecific peroxygenase (UPO) mutant 'PaDa-I' into the synthetic hydrogel polyethylene glycol diacrylate/ [2-(acryloxy)ethyl]trimethyl ammonia chloride (PEGDA/ AETMA) and its application as random packing material for flow biocatalysis (Fig. 1). The biocatalytic stereoselective oxygenation of alkylbenzenes by recombinant UPO has increased interest in recent years.[15a–c] Just recently, we holistically studied the carrier-bound immobilization of PaDa-I,[16] and could perform heterogenous oxyfunctionalizations in continuous operation.[17,18] To the best of our knowledge, we report here on the first example of continuous oxidations using a synthetic, 3D printable hydrogel as an immobilization matrix. We believe that our idea will enable a route to a mild 3D printing technique of a variety of enzymes. It could also allow access to novel enzyme containing reactors or enzymes immobilized in random packing material with high residual activity. Since the polymerization is based on photoinitiation, no elevated temperatures are used as in conventional 3D extruder printers. The methodology is hence suitable for many sensitive enzymes. In this paper, however, we have focused on the fundamental investigation of heterogenization (optimal enzyme amount, activity yield, and applicability). The follow-up 3D printing of the immobilized enzyme is ongoing and not the scope of this work.

We began our investigations on how we could achieve reproducible immobilization yields with the simultaneous production of unified immobilizates. To mimic the lithographic 3D printing process, we found that an exact amount of 10 μL aliquoted material solutions into 1.5 mL micro test tubes yielded consistent pellets after irradiation with UV light (365 nm for 3.5 min and afterward white light for 60 min, Fig. S1†). Before washing the pellets in buffer, they showed a mass of $10.0 \pm 0.4$ mg and a dimension of $1.4 \pm 0.1$ mm (height) times $3.9 \pm 0.1$ mm (diameter). After equilibrating the hydrogels pellets in buffer for 24 h, we determined a swelling degree $q_{m,\infty}$ of 7.6 and the pellet size was determined as $2.9 \pm 0.2$ mm (height) times $7.8 \pm 0.2$ mm

(diameter) with a mass of $85 \pm 5$ mg (compare Fig. S2, S7 and Table S3†).

After standardizing the method to produce the pellets, we investigated the immobilization of PaDa-I. Here, we studied two fundamentally different immobilization methods: (i) incubation of hydrogel pellets in the PaDa-I stock solution, and (ii) direct addition of the enzyme during the polymerization of the hydrogel (Fig. 1). However, the former method (i) showed significant enzyme leaching (data not shown), so the second approach was continued. To investigate the enzyme leaching, the enzyme-containing hydrogel pellets were washed three times in potassium phosphate buffer solution (KPi, 50 mmol L$^{-1}$, pH 7.0) and the washing fraction was analyzed with the ABTS assay (oxidation of 2,2′-azino-bis(3-ethylbenzothiazoline-6-sulfonic acid) for enzyme activity (Scheme S1†), and the Bradford assay for protein content. No protein in the washing fraction could be detected. However, a relatively high interference of the monomers of hydrogel matrix and the Bradford assay components was noticed. Yet, all absorbance values measured from the washing liquid of enzyme-loaded hydrogels were lower than that of the blank (= hydrogel pellet without enzyme). As an alternative attempt to determine the protein content, SDS-PAGE analysis showed no protein bands of the washing fractions (Fig. S3†). However, it should be noted that the sensitivity of the SDS gel analysis is relatively low; thus, for further studies we will use silver staining or quantitative western blotting to increase the sensitivity for enzyme leaching detection. The ABTS assay performed from each washing fraction showed negligible enzyme activity, in any case. Therefore, we concluded that no significant enzyme leaching occurs in the developed hydrogel-based heterogenization method. In a next step, we were interested in the residual activity of the enzyme hydrogel pellets and whether reusability of the material is possible. Mass specific activity of the immobilized enzyme was again measured via the standard ABTS assay in a thermostatic vessel with one hydrogel pellet. The mass specific activity in this study is defined as units per grams of wet carrier (= a gel that has
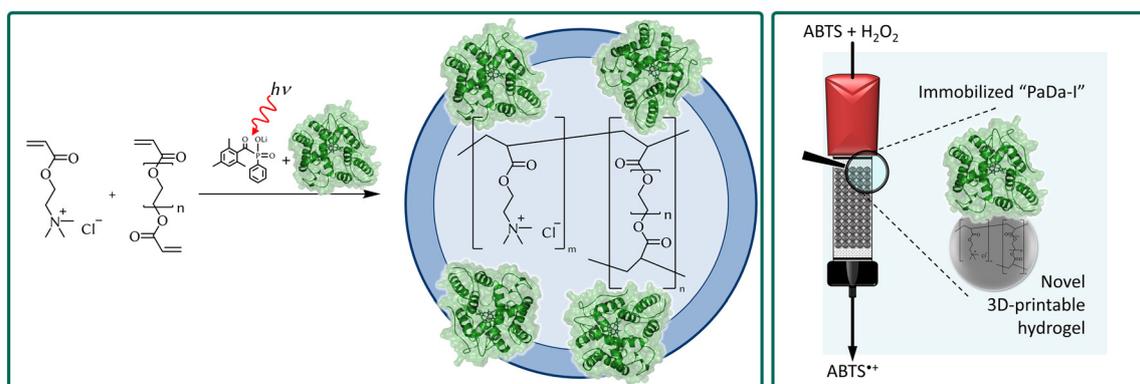


**Fig. 1** Concept of this work: synthesis of synthetic 3D printable hydrogels for enzyme immobilization (left). Application of novel heterogeneous enzyme as random packing material for continuous oxyfunctionalization synthesis oxidizing 2,2′-azino-bis(3-ethylbenzothiazoline-6-sulfonic acid) (ABTS).

been washed three times for each 1 hour before the activity assay was performed). The enzyme-loaded hydrogels pellets showed an activity of $3.2 \times 10^{-1}$ U $g_{wet\ carrier}^{-1}$ resulting in an activity yield of 6.1% (based on the mass of wet hydrogel carrier material). Subsequently, the enzyme hydrogel pellets were reused in two consequent cycles. In the second run (the first cycle), the activity dropped by 87% to $4.3 \times 10^{-2}$ U $g_{wet\ carrier}^{-1}$, and in the third run (the second cycle), the activity was only within the range of measurement accuracy (compare Fig. S6 and Table S2†). Therefore, it can be concluded that reuse – albeit limited – is possible for at least one cycle. The loss of activity could be explained by the fact that the enzyme on the surface of the particles was deactivated by the relatively harsh reaction condition of the ABTS assay. Subsequently, further investigations of the hydrogel-based immobilized UPO focused on additional aspects and are discussed here in short: (i) to achieve a generally higher activity, more enzyme was used in the pellets' synthesis. However, the activity remained the same in the standard error range (data not shown). (ii) The stirring speed was increased by a factor of two to avoid possible diffusion limitations, but no significant change in the activity was observed (Fig. S5 and Table S1†). (iii) The composition of the hydrogel matrix was changed by doubling or halving the amount of the crosslinker PEGDA (44 wt% or 11 wt%, respectively) to change the diameter of the inner pores. In this case, the activity of pellets with a denser polymer network showed no change compared with the standard enzyme–hydrogel pellets. Whereas looser networks provided *ca.* 66% lower activity values, significant leaching could not be detected (Fig. S8 and Table S4†). (iv) The pellet size was decreased by using half of the volume prior to polymerization (5 μL instead of 10 μL), hypothesizing that a higher surface would show increased activities. Nevertheless, no change of overall activity was observed (Fig. S9 and Table S5†).

As an interim conclusion, we demonstrated that the immobilization of UPO in the AETMA-PEGDA 700 hydrogel was successfully performed. Based on the activity and protein analysis of the washed fractions, no significant leaching of the immobilized PaDa-I was observed. It is hypothesized that the unfortunate poor reusability of the pellets is due to the restricted mass transfer, which limits the activity of the enzyme entrapped in the gel compared to that of immobilized at the gel surface. To improve the properties of the immobilized PaDa-I, various experimental parameters (*e.g.*, stirring speed, crosslinker amount, enzyme amount, pellet size) were evaluated in detail. Surprisingly, none of them could affect the increase of the activity of the immobilized biocatalyst leading to the conclusion that the method has already reached its optimum.

Next, the immobilized enzyme was applied in a biocatalytic continuous flow approach. A commercial Tricorn 10/50 column from Cytiva was used for the continuous flow experiments. The column was packed with the hydrogels containing the immobilized PaDa-I. Two processing strategies were here evaluated. In the first, 300 μL of the hydrogel was polymerized

directly in the column, creating a random hydrogel film packing. In the second, the column was filled with 30 pieces of hydrogel pellets, corresponding to the volume used for random film packing. To evaluate and compare both approaches, the ABTS model reaction system was used (Fig. 2). The key parameters of the applied bedding in the column were assessed as the following: volume of hydrogel applied: 300 mL; bed height: 5 cm; reactor volume: 3.9 mL; theoretical residence time of ABTS at a total flow rate of 0.5 mL min$^{-1}$: 7.9 min. In every experimental run, the column was washed with buffer for 30 minutes with a flow rate of 0.5 mL min$^{-1}$, which is the total wash volume used in washing the pellets. Afterwards, the system's UV detector was equilibrated with 0.3 mmol L$^{-1}$ ABTS solution for 10 min with a flow rate of 0.5 mL min$^{-1}$. All reactions were run overnight (*ca.* 1200–1500 min) with 0.496 mL min$^{-1}$ ABTS solution and 0.004 mL min$^{-1}$ hydrogen peroxide solution (0.035 wt%). In three individual experiments, the random hydrogel film packing generated an average continuous production of $2.2 \pm 1.6$ mg L$^{-1}$ of ABTS$^{\bullet+}$ yielding in an average space–time-yield (STY) of $0.017 \pm 0.013$ g L$^{-1}$ h$^{-1}$ (Table 1, entries 1–3). In three more individual experiments, the random pellet packing generated an average continuous production of $1.6 \pm 0.7$ mg L$^{-1}$ of ABTS$^{\bullet+}$ yielding in an average STY of $0.012 \pm 0.005$ g L$^{-1}$ h$^{-1}$ (Table 1, entries 1–3). Since these results are within the experimental error range of the previous experiment, it cannot be stated that one approach is better than the other one. Interestingly, the standard deviation was significantly reduced to 50%, proving that the packed pellets is more reliable and can provide more consistent results.
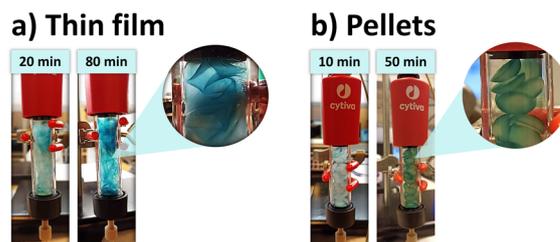


**Fig. 2** Using PaDa-I enzyme-loaded hydrogels as (a) a random thin film or (b) pellet packing for continuous flow biocatalysis. The blue color is resulted from trapped ABTS$^{\bullet+}$ into the hydrogel material.

**Table 1** Production of ABTS$^{\bullet+}$ and space–time-yield (STY) of thin film and pellet packing in continuous operation using hydrogel-based immobilized PaDa-I (also compare Fig. S4†). Each entry represents an individual experiment

| Entry | $c$(ABTS$^{\bullet+}$)/mg L$^{-1}$ | STY/g L$^{-1}$ h$^{-1}$ |
|---|---|---|
| *Thin film packing* | | |
| 1 | 0.86 | $6.6 \times 10^{-3}$ |
| 2 | 4.04 | $3.1 \times 10^{-2}$ |
| 3 | 1.60 | $1.2 \times 10^{-2}$ |
| *Pellet packing* | | |
| 4 | 2.28 | $1.7 \times 10^{-2}$ |
| 5 | 1.50 | $1.1 \times 10^{-2}$ |
| 6 | 0.94 | $7.2 \times 10^{-3}$ |

**986** | *React. Chem. Eng.*, 2023, **8**, 984–988

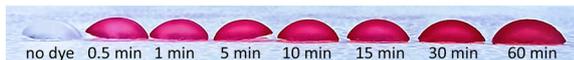This journal is © The Royal Society of Chemistry 2023

**Fig. 3** Profile of hydrogel pellets coloured with basic fuchsin over time.

Recently, we reported about the continuous PaDa-I production of ABTS[·+], where the enzyme was immobilized on commercially available carrier material ECR8315F from Purolite Lifetech.[17] In this previous study, we found an approximately 20-times higher production of ABTS[·+], and a 70-times higher STY in comparison with the here presented study. However, a fair comparison is not possible: The inherent advantage of our newly developed method allows the hydrogel material to be 3D printed in any conceivable shape. Therefore, the disadvantages could be overcome by an intelligent reactor design with miniatured well-defined channels. On the other hand, the hydrogels absorb a lot of water so that reactions in organic media are also possible. In addition, the hydrogels containing the enzyme could be easily stored at 4 °C for a couple of months without losing significant activity (data not shown). The free enzyme, however, showed approx. 35% loss of activity after 50 days being stored in the fridge at 4 °C.

Since it was hypothesized that the biocatalysis takes place mainly at the surface of the hydrogel, resulting in the relatively low activity, an attempt was made to investigate how quickly the substrate enters the hydrogel and how it is distributed throughout the pellet. In this experiment, seven empty hydrogel pellets were soaked in KPi buffer stained with basic fuchsin for different time periods. The first pellet was removed after 0.5 min, while the last one was stirred in the stained buffer for 60 min. Afterwards, the pellets were cut in half and compared with a reference (Fig. 3). An important detail that can be seen in the photo is the darker color stripes on the edge of the pellets. The longer the pellet remains in the colored buffer, the more intense its color becomes. However, even after 60 minutes, the darker band is clear and well visible. This finding is consistent with the theoretical model of liquid–solid mass transfer from bulk liquid media to porous supports. The image supports the hypothesis that the reaction occurs primarily at the surface of the hydrogels and that internal (pore) diffusion is a critical factor hindering the accessibility of the immobilized enzyme. Although the hydrogels could be vividly characterized from the images, quantitative evaluation was not possible due to the small size of the pellets.

## Conclusions

In this communication we presented for the first time in the literature a holistic immobilization procedure of the UPO mutant PaDa-I in a synthetic, 3D printable AETMA-PEGDA 700 hydrogel. The immobilization was carried out with an activity yield of 6.1%, which was two-times higher compared to covalently bound PaDa-I reported by us.[16] The activity and the protein content of the washing liquid was examined, and no leaching of the immobilized PaDa-I was determined. The reusability of the pellets proved to be relatively poor. An equilibrium swelling degree of 7.2 was found for the pellets being an essential measure for constructing the packed bed column.

Several experimental parameters were evaluated to be optimized (e.g., altering the (i) amount of enzyme immobilized, (ii) initial volume of the pellets, (iii) fabrication of pellets containing different weight percentages of crosslinkers, and (iv) testing the activity with higher agitation speed. None of these introduced positive changes for the activity of the immobilized enzyme. Using the model reaction of ABTS/ABTS[·+], the carrier containing the immobilized enzymes has been assessed in a continuous flow system, in the forms of random film and pellet packing. After optimizing the volume of the applied hydrogel, $2.2 \pm 1.6$ mg L$^{-1}$ and $1.6 \pm 0.7$ mg L$^{-1}$ of ABTS[·+] were produced with the film and the pellet packing, respectively. Ensuring greater control over the uniformity of the carrier, the latter showed more consistent results. However, the low performance of the immobilized enzyme reveals the challenge for future research: the enzyme in its immobilized form needs improvement in (i) residual enzyme activity, (ii) long-term process stability, and (iii) increased productivity. Our further studies will be dedicated to address these challenges. As regards future perspectives, there is a broad range of strategies that holds a promising solution for further research on this topic. To address the problem of mass transport in synthetic hydrogels, additive manufacturing could be a potential alternative, as it offers particularly great control over the product's structure, i.e., the possibility of producing a highly porous hydrogel material in the end. In addition, the encapsulation of different enzymes will also be investigated in the future. After implementing our findings for lithographic 3D printing, we believe that it will be possible to print specific reactor material with hyperfine pores to overcome the above-mentioned challenges.

## Author contributions

L.-E. Meyer and J. Meyer conceived the conception and design of this work. Method development was carried out by L.-E. Meyer. Experimental work was mainly carried out by D. Horváth and S. Vaupel. L.-E. Meyer and S. Kara were responsible for supervision, L.-E. Meyer and D. Horváth were responsible for validation, data curation, and visualization. S. Kara was responsible for funding acquisition and project administration. M. Alcalde provided the enzyme and contributed to project acquisition. L.-E. Meyer and D. Horváth wrote the original draft, and L.-E. Meyer, J. Meyer and S. Kara reviewed and edited the final draft. All authors agreed with the final version of the submitted manuscript.

## Conflicts of interest

There are no conflicts to declare.

This journal is © The Royal Society of Chemistry 2023

*React. Chem. Eng.*, 2023, **8**, 984–988 | **987**

# Acknowledgements

# Notes and references

1 (a) J. Coloma, Y. Guiavarc'h, P.-L. Hagedoorn and U. Hanefeld, Immobilisation and flow chemistry: tools for implementing biocatalysis, *Chem. Commun.*, 2021, **57**, 11416–11428; (b) P. De Santis, L.-E. Meyer and S. Kara, The rise of continuous flow biocatalysis – fundamentals, very recent developments and future perspectives, *React. Chem. Eng.*, 2020, **5**, 2155–2184; (c) A. I. Benítez-Mateos, M. L. Contente, D. Roura Padrosa and F. Paradisi, Flow biocatalysis 101: design, development and applications, *React. Chem. Eng.*, 2021, **6**, 599–611.

2 (a) M. M. C. H. van Schie, J.-D. Spöring, M. Bocola, P. Domínguez de María and D. Rother, Applied biocatalysis beyond just buffers - from aqueous to unconventional media. Options and guidelines, *Green Chem.*, 2021, **23**, 3191–3206; (b) S. Cantone, U. Hanefeld and A. Basso, Biocatalysis in non-conventional media—ionic liquids, supercritical fluids and the gas phase, *Green Chem.*, 2007, **9**, 954; (c) A. S. Bommarius and B. R. Riebel, in *Biocatalysis*, ed. A. S. Bommarius and B. R. Riebel, Wiley-VCH, Weinheim, 2005, pp. 339–372.

3 (a) J. M. Bolivar, J. M. Woodley and R. Fernandez-Lafuente, Is enzyme immobilization a mature discipline? Some critical considerations to capitalize on the benefits of immobilization, *Chem. Soc. Rev.*, 2022, **51**, 6251–6290; (b) L.-E. Meyer, M. Hobisch and S. Kara, Process intensification in continuous flow biocatalysis by up and downstream processing strategies, *Curr. Opin. Biotechnol.*, 2022, **78**, 102835; (c) P. Žnidaršič-Plazl, Biocatalytic process intensification via efficient biocatalyst immobilization, miniaturization, and process integration, *Curr. Opin. Green Sustainable Chem.*, 2021, **32**, 100546.

4 (a) J. Claus, A. Brietzke, C. Lehnert, S. Oschatz, N. Grabow and U. Kragl, Swelling characteristics and biocompatibility of ionic liquid based hydrogels for biomedical applications, *PLoS One*, 2020, **15**, e0231421; (b) N. Rekowska, J. Huling, A. Brietzke, D. Arbeiter, T. Eickner, J. Konasch, A. Riess, R. Mau, H. Seitz, N. Grabow and M. Teske, Thermal, Mechanical and Biocompatibility Analyses of Photochemically Polymerized PEGDA$_{250}$ for Photopolymerization-Based Manufacturing Processes, *Pharmaceutics*, 2022, **14**, 628.

5 J. Claus, A. Jastram, E. Piktel, R. Bucki, P. A. Janmey and U. Kragl, Polymerized ionic liquids-based hydrogels with intrinsic antibacterial activity: Modern weapons against antibiotic-resistant infections, *J. Appl. Polym. Sci.*, 2021, **138**, 50222.

6 D. L. Taylor and M. in Het Panhuis, Self-Healing Hydrogels, *Adv. Mater.*, 2016, **28**, 9060–9093.

7 A. Jastram, J. Claus, P. A. Janmey and U. Kragl, Rheological properties of hydrogels based on ionic liquids, *Polym. Test.*, 2021, **93**, 106943.

8 J. Romischke, A. Scherkus, M. Saemann, S. Krueger, R. Bader, U. Kragl and J. Meyer, Swelling and Mechanical Characterization of Polyelectrolyte Hydrogels as Potential Synthetic Cartilage Substitute Materials, *Gels*, 2022, **8**, 296.

9 J. Thiele, Y. Ma, S. M. C. Bruekers, S. Ma and W. T. S. Huck, 25th anniversary article: Designer hydrogels for cell cultures: a materials selection guide, *Adv. Mater.*, 2014, **26**, 125–147.

10 M. Maier, C. P. Radtke, J. Hubbuch, C. M. Niemeyer and K. S. Rabe, On-Demand Production of Flow-Reactor Cartridges by 3D Printing of Thermostable Enzymes, *Angew. Chem., Int. Ed.*, 2018, **57**, 5539–5543.

11 F. Croci, J. Vilím, T. Adamopoulou, V. Tseliou, P. J. Schoenmakers, T. Knaus and F. G. Mutti, Continuous flow biocatalytic reductive amination by co-entrapping dehydrogenases with agarose gel in a 3D-printed mould reactor, *ChemBioChem*, 2022, **23**, e202200549.

12 L. Wenger, C. P. Radtke, E. Gerisch, M. Kollmann, C. M. Niemeyer, K. S. Rabe and J. Hubbuch, Systematic evaluation of agarose- and agar-based bioinks for extrusion-based bioprinting of enzymatically active hydrogels, *Front. Bioeng. Biotechnol.*, 2022, **10**, 928878.

13 J. Wang, S. Stanic, A. A. Altun, M. Schwentenwein, K. Dietliker, L. Jin, J. Stampfl, S. Baudis, R. Liska and H. Grützmacher, A highly efficient waterborne photoinitiator for visible-light-induced three-dimensional printing of hydrogels, *Chem. Commun.*, 2018, **54**, 920–923.

14 J. Meyer, L.-E. Meyer and S. Kara, Enzyme immobilization in hydrogels: A perfect liaison for efficient and sustainable biocatalysis, *Eng. Life Sci.*, 2022, **22**, 165–177.

15 (a) M. Hobisch, D. Holtmann, P. Gomez de Santos, M. Alcalde, F. Hollmann and S. Kara, Recent developments in the use of peroxygenases - Exploring their high potential in selective oxyfunctionalisations, *Biotechnol. Adv.*, 2020, 107615; (b) A. Kinner, K. Rosenthal and S. Lütz, Identification and Expression of New Unspecific Peroxygenases - Recent Advances, Challenges and Opportunities, *Front. Bioeng. Biotechnol.*, 2021, **9**, 705630; (c) M. Kluge, R. Ullrich, K. Scheibner and M. Hofrichter, Stereoselective benzylic hydroxylation of alkylbenzenes and epoxidation of styrene derivatives catalyzed by the peroxygenase of *Agrocybe aegerita*, *Green Chem.*, 2012, **14**, 440–446.

16 P. De Santis, N. Petrovai, L.-E. Meyer, M. Hobisch and S. Kara, A holistic carrier-bound immobilization approach for unspecific peroxygenase, *Front. Chem.*, 2022, **10**, 985997.

17 L.-E. Meyer, B. Fogtmann Hauge, T. Müller Kvorning, P. De Santis and S. Kara, Continuous oxyfunctionalizations catalyzed by unspecific peroxygenase, *Catal. Sci. Technol.*, 2022, **12**, 6473–6485.

18 M. Hobisch, P. De Santis, S. Serban, A. Basso, E. Byström and S. Kara, Peroxygenase-Driven Ethylbenzene Hydroxylation in a Rotating Bed Reactor, *Org. Process Res. Dev.*, 2022, **26**, 2761–2765.